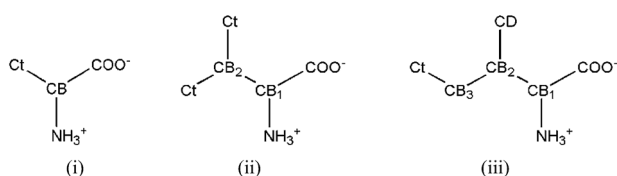




maladies were reported.<sup>17,20,25–29</sup> Actually,  $\text{Al}^{3+}$  has been recognized as a neurotoxic agent and its possible role in Alzheimer's disease and other neurodegenerative disorders<sup>28,29</sup> has been actively investigated. It has been shown that enhanced  $\text{Al}^{3+}$  levels are likely to influence the structure and function of nerve cells proteins by promoting aggregation of neural molecules or by interfering with a large number of neurochemical reactions.<sup>16,26,28,29</sup> With the increasing bioavailability of this metal ion due to acid rain witnessed in the last decades, the study of the relationship between its levels in biological fluids, and tissues and its potential involvement in neurological disorders, has gained a renewed interest.<sup>25,27</sup> In most natural systems, the aluminum absorption, excretion, tissue retention and deposition will depend on the properties of the  $\text{Al}^{3+}$  complexes formed with biological ligands.<sup>27</sup> Despite the efforts, however, the identity of these complexes in biological media has not yet been established.

Recently, based on novel evidence provided by solubility and simulation data, we proposed a mechanism for the action of salting-in inducing cations in aqueous solutions of amino acids.<sup>14</sup> Even though remarkable progresses have been made, there are still a number of key questions concerning the cations operation mechanism upon the solubility of biomolecules that remain unsolved. In order to further delve into the molecular scenario behind the cation specific effects, and in particular their dependence on the charge of the ions, thermodynamic and molecular dynamics (MD) simulation methods are here used to study the interactions between amino acids and mono-, di- and trivalent cations in aqueous media, with special emphasis on the aluminum ion. With that aim, novel experimental solubility measurements and MD simulations were carried out for aqueous solutions of three amino acids – alanine (Ala), valine (Val) and isoleucine (Ile), depicted in Fig. 1, in presence of the chloride and sulfate salts of  $\text{K}^+$ ,  $\text{Li}^+$ ,  $\text{Ca}^{2+}$  and  $\text{Al}^{3+}$  cations, at  $T = 298.15$  K. The amino acids are here used as model compounds and the ions were selected in order to span a representative range of charges, from mono to polyvalent cations with biological relevance. Since physiological environments are very often neutral, most of the solubility measurements were performed in a pH range close to the isoelectric point, and therefore only the zwitterionic forms of the solutes were considered in the simulations.

Despite the large amount of reports on the solubility and stability of amino acids and proteins in presence of salts,<sup>14,30–43</sup> the solubility data available for the systems under study is



**Fig. 1** Structure and atom labeling of the amino acids studied in this work: (i) alanine (Ala), (ii) valine (Val) and (iii) isoleucine (Ile).  $\text{C}_t$  stands for the terminal carbon atom of the amino acid side chain and  $\text{C}_B$  ( $x = 1, 2, 3$ ) for the other carbon atoms of the same alkyl chain. Hydrogen atoms bonded to carbon are omitted for clarity.

scarce and/or contradictory, not to mention the paucity of systematic theoretical investigations. In this work, the analysis of the results derived from the computational studies will provide an explanation for the solubility behavior experimentally observed for the aqueous solutions of the amino acids and salts here considered.

## 2. Experimental section

### 2.1. Chemicals

The source and purity of the chemical compounds used are given in Table 1. The amino acids were kept at room temperature, and used without further purification. Lithium chloride and potassium sulfate were oven-dried (about 350 K) during at least 24 h, and used after cooling at room temperature in a dehydrator with silica gel to avoid water contamination by air humidity. The distilled water was cleaned in a milli-Q ultra-pure water system from Millipore.

### 2.2. Experimental procedure

The solubility experiments were carried out using the analytical isothermal ( $\pm 0.1$  K) shake-flask method as described in our previous work<sup>14</sup> and so, only a short description is here provided concerning the quantitative analysis carried out by three different methods: gravimetry, densimetry or refractive index measurements, selected considering the type of the salt and solubility level. Either using gravimetry or densimetry, at least three samples of about  $5 \text{ cm}^3$  of the saturated liquid phase were collected using previously heated plastic syringes coupled with polypropylene filters ( $0.45 \mu\text{m}$ ).

The gravimetric method was selected for mixtures with  $\text{K}_2\text{SO}_4$ , which does not form hydrated phases. Therefore, the samples were placed into pre-weighed ( $\pm 0.1$  mg) glass vessels and immediately weighed. Then, all the solvent was evaporated, and the crystals dried completely in a drying stove at 343.15 K for 3 days. Finally, the glass vessels were cooled in a dehydrator with silica gel for one day and weighed. The process was regularly repeated until a constant mass was achieved.

For aqueous solutions containing  $\text{LiCl}$ ,  $\text{Li}_2\text{SO}_4$ , or  $\text{CaCl}_2$ , density measurements were performed using a vibrating tube

**Table 1** Specifications of the chemicals used

Chemical name	Supplier	Minimum mass fraction purity <sup>a</sup>
DL Alanine	Merck	0.99
L Valine	Merck	0.99
L Isoleucine	Merck or Fluka	0.99
Aluminium chloride hexahydrate	Merck	0.97
Aluminium sulfate octadecahydrate	VWR chemicals	0.96
Calcium chloride dehydrate	Merck	0.99
Lithium chloride	Merck	0.99
Lithium sulfate monohydrate	Merck	0.99
Potassium sulfate	Panreac	0.99

<sup>a</sup> Declared by the supplier.

digital density meter (DMA 5000 M, Anton Paar) with a reproducibility within  $\pm 3 \times 10^{-3} \text{ kg m}^{-3}$ . Firstly the calibration curve ( $r^2 > 0.999$ ), relating the amino acid concentration (in  $\text{g kg}^{-1}$  of water) and the density was built, preparing six standard solutions of known composition. The samples were discharged into glass vessels containing a known weighed amount (between 12 to 15 g) of binary salt aqueous solution at the same salt molality as the ternary saturated solution. After mixing, densities were measured following standard procedures, and converted to the solubility.

A third method was adapted from the work by Venkatesu *et al.*,<sup>44</sup> and applied to aqueous solutions containing aluminum salts. Twelve vials were prepared adding different amounts of amino acid, and approximately the same volume of aqueous solution, of a given salt molality. The mass of amino acid was chosen in order that about 6 samples result in saturated solutions and, the remaining non-saturated. These solutions were subject exactly to the same stirring and settling times, as in the previous methods, but the volume of each sample is now  $1 \text{ cm}^3$ . After, the refractive index of these twelve samples was measured (Abbemat 500, Anton Paar) with a reproducibility within  $\pm 1 \times 10^{-5}$ . Plotting the refractive index *versus* the amino acid content, two linear curves are found, for which their intersection represents the solubility value.

### 2.3. Computational methods

MD calculations were performed for aqueous solutions of the zwitterionic forms of the amino acids (pH = 7) at a concentration of approximately  $0.35 \text{ mol dm}^{-3}$  in the presence of the salts. A concentration of  $1.0 \text{ mol dm}^{-3}$  was selected for all the salts, except for  $\text{K}_2\text{SO}_4$  for which a concentration of  $0.50 \text{ mol dm}^{-3}$  was considered, due to its lower aqueous solubility. The simulations were carried out using the isothermal-isobaric  $NpT$  ( $T = 298.15 \text{ K}$  and  $p = 1 \text{ bar}$ ) ensemble and the GROMACS 4.04 molecular dynamics package.<sup>45</sup> The equations of motion were integrated with the Verlet–Leapfrog algorithm<sup>46</sup> and a time step of 2 fs. The Nosé–Hoover thermostat<sup>47,48</sup> was used to fix the temperature, while the Parrinello–Rahman barostat<sup>49</sup> was employed to fix the pressure. Starting configurations were generated in cubic boxes with lateral dimensions of 45 Å, and periodic boundary conditions were applied in three dimensions. The systems were prepared by randomly placing amino acids, ions and water molecules in the simulation box. Six amino acid molecules were included in each box, solvated by 900 water molecules. Seventeen cation–anion pairs were incorporated to obtain the 1.0 M salt concentration; in the case of  $\text{K}_2\text{SO}_4$ , boxes with 9 cation–anion pairs were used to obtain a 0.5 molarity. Then, a 10 000 step energy minimization was performed and followed by two simulations, the first one with 50 000 steps for equilibration and the final one with 10 000 000 steps for production (*i.e.*, total production time of 20 ns). After equilibration, the values of the box volume ranged between 27.8 to 29.9  $\text{nm}^3$ , depending on the system. Equilibration was checked ensuring that all observables (including the RDFs) fluctuated around their equilibrium values during the production stage.

The intermolecular interaction energy between pairs of neighboring atoms was calculated using the Lennard-Jones potential to describe dispersion/repulsion forces and the point-charge Coulomb potential for electrostatic interactions. Long-range electrostatic interactions were accounted using the particle-mesh Ewald method,<sup>50</sup> with a cutoff of 1.0 nm for the real-space part of the interactions. A cutoff radius of 1.2 nm was used for the Lennard-Jones potential, and long-range dispersion corrections were added to both energy and pressure. All bond lengths were held rigid using the LINCS constraint algorithm,<sup>51</sup> while angle bending was modeled by a harmonic potential and dihedral torsion was described (where appropriate) by a Ryckaert–Bellemans function. Potentials available in the literature were taken for all the species considered in the simulations. Water was described by the rigid SPC/E model,<sup>52</sup> while the OPLS all-atom potential was applied for the amino acids<sup>53</sup> and for the chloride, lithium, calcium and potassium ions.<sup>53,54</sup> For sulfate, the force field parameters of the second (std2) model proposed by Cannon *et al.*<sup>55</sup> were used, and for the aluminum cations the force field parameters were taken from the work of Faro *et al.*<sup>56</sup> The force fields selected for the ions in this work have provided accurate description of aqueous saline solutions of amino acids,<sup>13,14</sup> and it has been shown that although absolute degrees of binding are somehow affected by the choice of the model, relative changes along the Hofmeister series are unchanged.<sup>13</sup> Nevertheless, Heyda *et al.*<sup>57</sup> demonstrated that the consideration of non-polarizable and polarizable models for describing the interaction of halides with basic amino acids (Arg, His and Lys) in water leads to similar conclusions, *i.e.*, water densities around the charged regions and the ion-specific interactions for charged and apolar regions of those amino acids were qualitatively the same.

Radial distribution functions (RDFs) for several atomic pairs were sampled during the production stage using the `g rdf` tool of GROMACS.

## 3. Results and discussion

### 3.1. Experimental

The solubilities of the amino acids in the aqueous solutions of the different salts, measured at various electrolyte concentrations and 298.15 K, are presented in Tables 2 and 3, together with the standard deviation (in brackets). The maximum coefficient of variation is 1.97%. Fig. 2 shows the relative solubility, expressed as the ratio between the solubility of the amino acid in the electrolyte solution to that in pure water, for the three amino acids in the aqueous saline solutions of  $\text{LiCl}$ ,  $\text{Li}_2\text{SO}_4$ ,  $\text{K}_2\text{SO}_4$  and  $\text{CaCl}_2$ .

Both increases (salting-in) and decreases (salting-out) of the amino acid aqueous solubilities are observed with the increase of the electrolyte concentration, being the most pronounced solubility effects induced by the salts comprising the polyvalent cations. As can be seen in Fig. 2(a),  $\text{LiCl}$  does not have a significant influence on the aqueous solubilities of the amino acids studied. Nevertheless, for higher molalities of the salt, a slight salting-out effect is observed in the case of Ile. As shown in Fig. 2(b),  $\text{Li}_2\text{SO}_4$  and  $\text{K}_2\text{SO}_4$  promote salting-out of Val and Ile

in the entire molality range, an effect more pronounced for isoleucine. In the case of alanine, a slight salting-in effect is observed at low electrolyte concentrations, followed by a decrease in solubility for higher molalities of  $K_2SO_4$ .

The behavior of the salts of the polyvalent cations is the opposite of that observed for the electrolytes comprising the monovalent cations. As shown in Fig. 2(a), calcium chloride induces a strong salting-in of all the amino acids studied, which is more significant for Ala than for Val and Ile. Indeed, the  $Ca^{2+}$  cation is a strong salting-in agent (*cf.* Table 2), with a behavior very similar to that of  $Mg^{2+}$ .<sup>14</sup>  $Al^{3+}$  exhibits a more remarkable effect, as both aluminum salts promote an exceptionally strong salting-in, with a relative solubility varying from 2.40 to 2.85 (*cf.* Table 3). In fact, a salt molality of 0.5 is sufficient to promote a large increase in the aqueous solubilities of the amino acids, while, in the other systems, considerably higher salt molality is not enough to trigger this effect.

The results obtained in this work for  $K_2SO_4$  and  $CaCl_2$  were compared with data available in the literature (Fig. 3). The scarcity of solubility data did not enable a comparison for the other systems. As shown in Fig. 3(b), the solubility of DL-alanine in  $CaCl_2$  aqueous solutions compares well with the results reported by El-Dossoki *et al.*,<sup>39</sup> but suggests very different trends for higher molalities. A more evident disagreement is observed

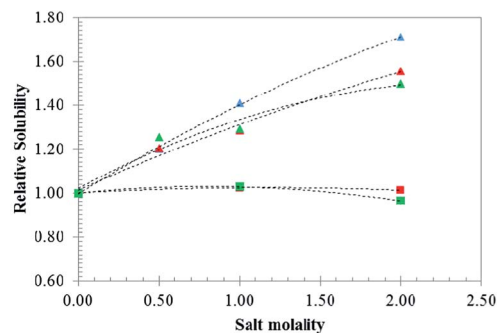
**Table 2** Amino acid solubility ( $g\ kg^{-1}$  of water) at  $T = 298.15\ K$  and different salt molalities

$K_2SO_4$ molality	DL Alanine	L Isoleucine	L Valine
0.00	164.67 (0.05)	34.625 <sup>a</sup> (0.137)	57.893 (0.031)
0.20	168.19 (0.01)	33.727 (0.049)	56.930 (0.070)
0.40	167.55 (0.14)	31.671 (0.380)	53.950 (0.093)
0.50	166.54 (0.06)	30.327 (0.163)	52.272 (0.169)
<b>CaCl<sub>2</sub> molality</b>			
0.00	164.67 (0.05)	33.442 <sup>b</sup> (0.036)	57.893 (0.031)
0.50	198.58 (0.05)	41.971 (0.117)	69.794 (0.100)
1.00	232.75 (0.10)	43.215 (0.807)	74.381 (0.078)
2.00	283.14 (0.93)	50.099 (0.462)	90.110 (0.558)

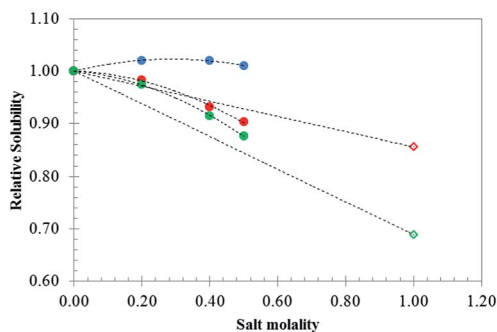
<sup>a</sup> Supplied by Fluka. <sup>b</sup> Supplied by Merck.

**Table 3** Amino acid solubility ( $g\ kg^{-1}$  of water) at  $T = 298.15\ K$  and different salt molalities

LiCl molality	L Isoleucine	L Valine
0.00	33.442 (0.036)	57.893 (0.031)
1.00	34.365 (0.088)	59.279 (0.045)
2.00	32.217 (0.077)	58.579 (0.123)
<b>Li<sub>2</sub>SO<sub>4</sub> molality</b>		
1.00	23.043 (0.045)	49.530 (0.065)
<b>AlCl<sub>3</sub> molality</b>		
0.50	95.457 (0.633)	138.93 (1.025)
<b>Al<sub>2</sub>(SO<sub>4</sub>)<sub>3</sub> molality</b>		
0.50	81.736 (1.609)	142.02 (1.810)



(a)



(b)

**Fig. 2** Relative solubility of alanine (blue), valine (red), and isoleucine (green) in aqueous solutions, at 298.15 K, containing the salt: (a)  $\square$ , LiCl;  $\Delta$ ,  $CaCl_2$ ; and in (b)  $\diamond$ ,  $Li_2SO_4$ ;  $\circ$ ,  $K_2SO_4$ . Lines are guides to the eyes.

in Fig. 3(a), where the pronounced salting-in effect of potassium sulfate, reported by the author<sup>39</sup> is not confirmed by the data measured in this work. It must be pointed out that this author presents amino acid solubility at a potassium sulfate molality above its solubility limit in water, and so data from El-Dossoki<sup>39</sup> need to be carefully checked as some other significant discrepancies have been found. For instance, studying the  $Na_2SO_4$  effect on the aqueous solubility of DL-alanine at 298.15 K and for salt molality equal to one, Ramasami<sup>35</sup> found a relative solubility of 0.960, while Ferreira *et al.*<sup>36</sup> measured 0.964, both indicating a smooth salting-out, but for the same conditions El-Dossoki<sup>39</sup> gives a relative solubility of 1.689, which is a considerable salting-in effect.

Nevertheless, the previous experience of the authors on this type of measurements,<sup>14,36,38</sup> the low standard deviations observed, the high reliability of the amino acid solubility in water, and the analysis of the simulation data presented below, all support the quality of the results provided in the current study.

The pH was also measured (inoLab pH 720, WTW) at 298.15 K for some selected saturated amino acid solutions, which are given in Table S1 (*cf.* ESI<sup>†</sup>). Excepting for aluminum salts, the pH introduces a minor effect on the solubility change as it varies from pH = 5.69 in a saturated solution of valine (in  $CaCl_2$ ) to pH = 6.11 in a saturated valine aqueous 1 molal  $Li_2SO_4$  solution, very close to the isoelectric point where the amino acid is in its zwitterionic form.<sup>58</sup>

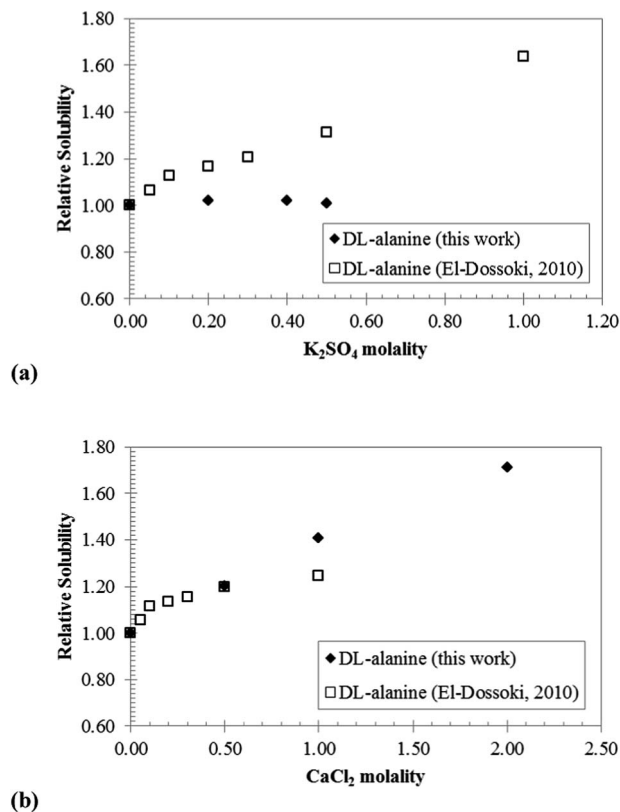


Fig. 3 Comparing relative solubility of DL-alanine aqueous electrolyte solutions at 298.15 K: (a)  $K_2SO_4$  and (b)  $CaCl_2$ .

### 3.2. MD simulations

To understand the specific effects of the cations on the aqueous solubilities of the amino acids experimentally observed, radial distribution functions were calculated for all the possible interactions involving the amino acid constituting groups (Fig. 1), the cations, the anions, and water. These RDFs provide a quantitative description of enhancement (values larger than 1) or depletion (values smaller than 1) of densities of species around a selected moiety. The most relevant RDFs are presented in the main body of the paper, while additional plots are provided as ESI.† Values for the position and intensities of the RDF peak maxima for selected systems are also given as ESI.† The MD results here reported were obtained for the zwitterionic forms of the amino acids. Furthermore, the MD calculations for the  $K_2SO_4$  systems were performed for a different concentration of the salt. Even though the concentration is likely to affect the intensity of the RDF peaks, this is not, as it will be seen, relevant for the global interaction patterns discussed.

**The effect of the charge of the cation.** To evaluate the influence of the charge and nature of the cation, we begin by considering the results obtained for the RDFs corresponding to the interactions of the cations considered in this work with the atoms representative of the nonpolar and of the negatively charged groups of Ile.

Fig. 4 shows the RDFs corresponding to the interactions of the cations with  $C_t$  and  $C_B$  atoms of Ile (representative of the nonpolar part of the amino acid). As suggested by the intensity

and position of the peaks (please also refer to Table S2, cf. ESI†), these interactions are absent in presence of the salts of the monovalent lithium and potassium ions, and occur only at a second solvation layer for the systems comprising the polyvalent  $Ca^{2+}$  and  $Al^{3+}$ . In the case of the latter, the strongest RDF peaks referring to the contact pairs ( $C_t/C_B \cdots cation$ ) are observed for aqueous solutions of  $AlCl_3$ , and the weakest for  $Al_2(SO_4)_3$ . Both occur, though, for shorter distances than in the case of  $CaCl_2$ . The RDFs for the association of the cations with  $C_B$  of Ile are more intense than those for  $C_t$ , indicating a stronger binding to the former, very likely because  $C_B$  is closer to the charged  $COO^-$  group.

In Fig. 5, the RDFs of the cations around the oxygen atom of the carboxyl group of Ile are displayed. The first remarkable result is that the mono and the polyvalent cations present totally distinct behaviors. While the binding of the polyvalent cations to the negatively charged group of the amino acid is extremely strong, the  $O(COO^-)$ -monovalent cation interactions are by far much weaker. Indeed, as can be seen in Fig. 5(b) and Table S2,† the RDF peaks corresponding to the interactions of  $Al^{3+}$  and  $Ca^{2+}$  with the oxygen atoms of the carboxyl group of Ile are

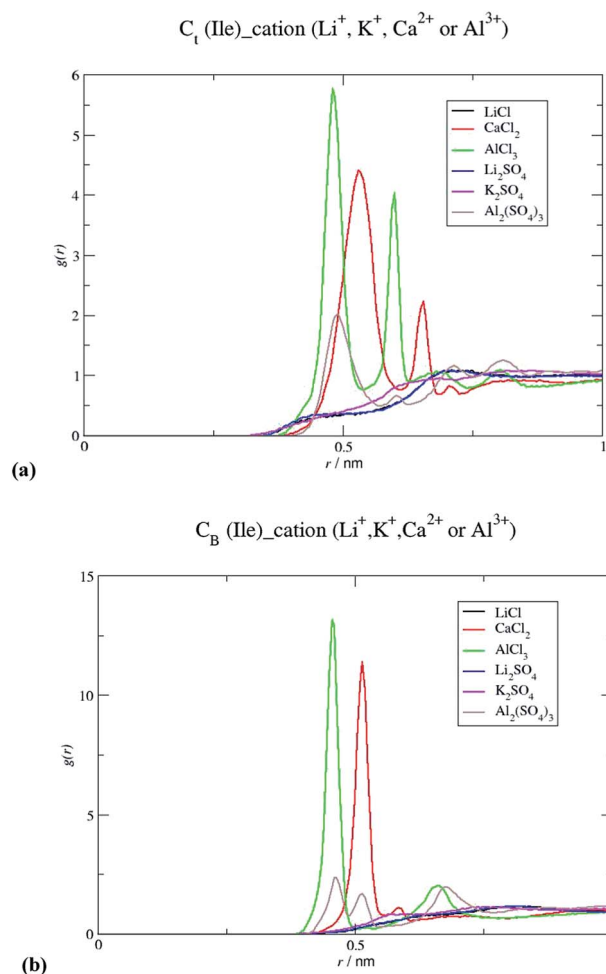


Fig. 4 Radial distribution functions for the interactions between the cations and the nonpolar regions of Ile: (a) terminal carbon and (b) bone carbon.

extremely intense and occur for very short distances, particularly in the case of  $\text{Al}^{3+}$ , for which an exceptionally significant structuring around  $\text{COO}^-$  is observed. Their strengths decrease in the order  $\text{AlCl}_3 > \text{Al}_2(\text{SO}_4)_3 > \text{CaCl}_2$ . In contrast, the distribution of the monovalent cations around the  $\text{COO}^-$  group of the amino acid (Fig. 5(a)) does not reveal the presence of the lithium ion in the vicinity of the negatively charged group, and suggests some, yet rather weak, association of  $\text{K}^+$ .

This molecular picture can be better visualized from the snapshots obtained from simulations of aqueous solutions of Ile in the presence of lithium and aluminum salts, depicted in Fig. 6, 7, S1 and S2 (*cf.* ESI†) showing the relative positions of the ions around the carboxyl group, and remarkably shorter distances in the case of  $\text{Al}^{3+}$  than  $\text{Li}^+$ .

The spatial distribution functions (SDFs) calculated for Ile systems comprising  $\text{Li}^+$ ,  $\text{Ca}^{2+}$  and  $\text{Al}^{3+}$  chloride salts are as well illustrative of the molecular scenario described. As can be seen in Fig. 8, the SDF region for the aluminum cation is located quite near the carboxyl group, and become further and more diffuse as one moves to calcium and, more remarkably, to  $\text{Li}^+$  cations, suggesting the pronounced preference of  $\text{Al}^{3+}$  for the negatively charged group of the amino acid. The patterns of the interactions described for Ile are also observed for Ala (Fig. S3,

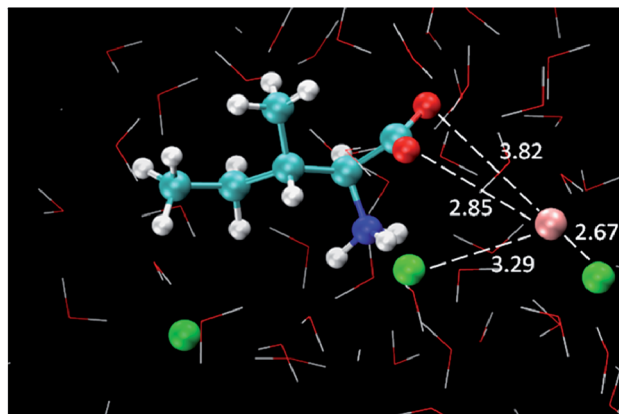


Fig. 6 Snapshot from a simulation of (Ile + LiCl + water) mixtures, showing the distances (Å) between selected atoms. Light blue spheres represent carbon atoms, dark blue spheres are nitrogen atoms, red spheres are oxygen atoms, white spheres are hydrogen atoms, green spheres are chloride anions and pink spheres are lithium cations. Water molecules are represented in line style.

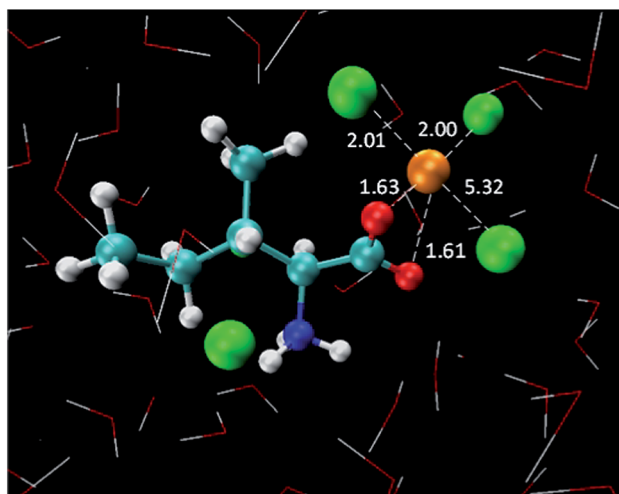


Fig. 7 Snapshot from a simulation of (Ile +  $\text{AlCl}_3$  + water) mixtures, showing the distances (Å) between selected atoms. Light blue spheres represent carbon atoms, dark blue spheres are nitrogen atoms, red spheres are oxygen atoms, white spheres are hydrogen atoms, green spheres are chloride anions and orange spheres are aluminum cations. Water molecules are represented in line style.

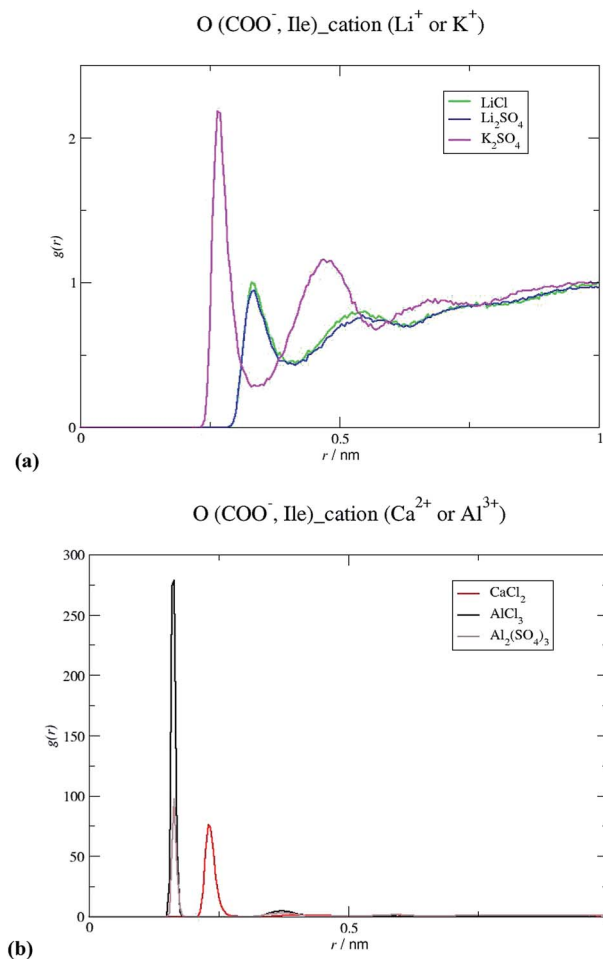
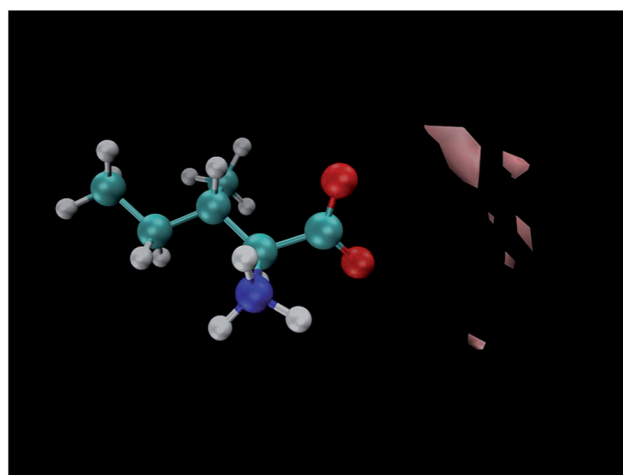


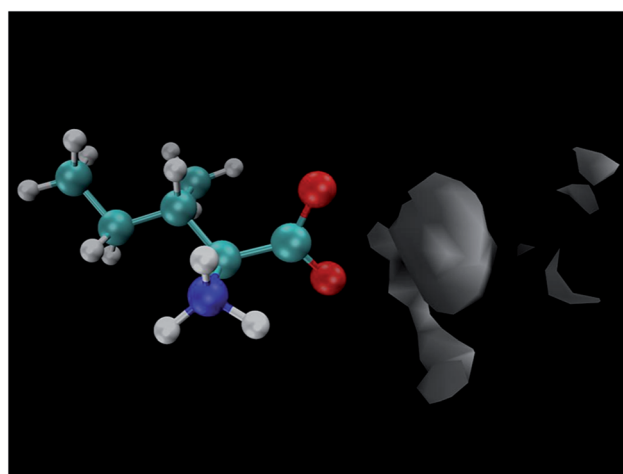
Fig. 5 Radial distribution functions for the interactions between the (a) monovalent and (b) polyvalent cations and the carboxyl group of Ile.

*cf.* ESI†) and for Val (Fig. S4, *cf.* ESI†), being the slight differences found among the amino acids related to the effect of the size of the alkyl side chain.

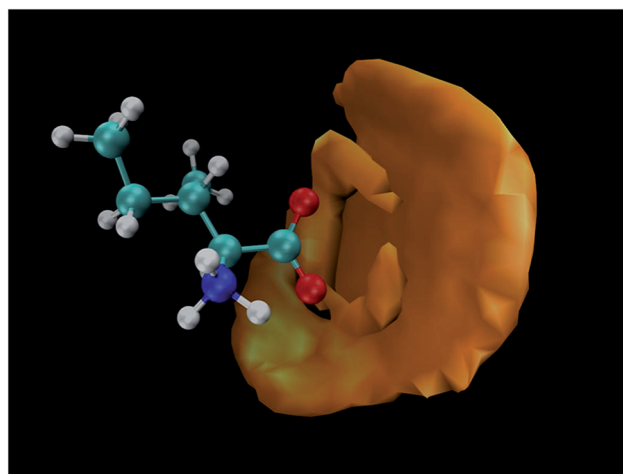
Aiming at disclosing the nature of the strong  $\text{O}(\text{COO}^-)$ –polyvalent cation interactions, we analyzed the thermodynamic properties of hydration of the ions (Table 4), as well as literature data available. As can be seen in Table 4, the  $\text{Ca}^{2+}$  and  $\text{Al}^{3+}$  ions present large energies of hydration<sup>59</sup> and should therefore form hydration complexes that would contribute to the dehydration of the amino acids and their salting-out, as it happens with other molecules such as ionic liquids<sup>60</sup> and proteins.<sup>40,42</sup> That is not, however, experimentally observed in this work. Instead, as shown in Fig. 2 and Tables 2 and 3, calcium and aluminum salts



(a)



(b)



(c)

Fig. 8 Spatial distribution functions (SDFs) for the lithium (pink), calcium (grey) and aluminum (orange) ions around the carboxyl group of Ile in (a) (Ile + LiCl + water); (b) (Ile + CaCl<sub>2</sub> + water) and (c) (Ile + AlCl<sub>3</sub> + water) mixtures. Color code for the explicitly represented atoms is the same as Fig. 6.

behave as strong salting-in agents, in agreement with the solubility effects observed for other biomolecules such as polymers,<sup>61</sup> charged polypeptides<sup>62</sup> and amino acids.<sup>40</sup> Polyvalent cations have well recognized specific binding to a diversity of biomolecules, and are known to stabilize a variety of protein structures.<sup>18,19,21 23,26,29,63 65</sup> It is well recognized, for instance, that divalent ions such as magnesium and calcium are able to form complexes with amino acids and proteins in aqueous solutions, specially with negatively charged residues, with oxygen being the favorite coordinating atom.<sup>18,63 65</sup> Furthermore, aluminum is known to form fairly stable complexes with negatively charged O-donor chelating biomolecules, including amino acids<sup>22,23,26,29</sup> and other carboxylate, catecholate and phosphate ligands.<sup>19,21,29</sup> More specifically, the important role of the carboxyl group in the interactions established in multicomponent biochemical systems, and the idea that the ions interact directly with the biocompounds, has been pointed out several times.<sup>12,14,22,26</sup> For these reasons, the strong association of the polyvalent cations to the negatively charged group of the amino acids, revealed by the RDFs calculated in this work, actually suggests the formation of a complex of the cation with the biomolecules.

It is worth to analyze in more detail the particular case of the aluminum ion. The much more pronounced structuring of this cation around COO<sup>-</sup> when compared to the divalent cations (Fig. 5, S3 and S4<sup>†</sup>) and the more significant salting-in effects observed for the Al<sup>3+</sup> salts (Table 3) would, in this context, suggest the formation of extremely stable (amino acid-cation) chelates. There are, however, a number of additional factors that must be taken into account. Although the highly polarizing potential of Al<sup>3+</sup> dictates indeed a particular affinity of this ion for oxygen donors such as carboxylate groups,<sup>19</sup> the understanding of the mechanisms that govern the formation of aluminum ligands with biomolecules requires a deep knowledge of the speciation of this metal.<sup>25,27</sup> The aluminum cation has a high tendency to suffer hydrolysis, leading to the formation of a variety of mono and polynuclear hydroxo complexes, and eventually still larger oligomeric species. The distribution of these hydrolysis products, strictly dependent on the media conditions, will play an essential role on the coordination/chelating properties of this cation. Unfortunately, an accurate description of aluminum complexation equilibria and kinetics has been quite hard to establish.<sup>25,27</sup> Though the characterization

Table 4 Molar entropy of hydration,  $\Delta_{\text{hyd}}S$ , Gibbs free energy of hydration,  $\Delta_{\text{hyd}}G$ , and enthalpy of hydration,  $\Delta_{\text{hyd}}H$ , at 298.15 K, for the ions studied in this work<sup>a</sup>

Ion	$\Delta_{\text{hyd}}S/\text{J K}^{-1} \text{mol}^{-1}$	$\Delta_{\text{hyd}}G/\text{kJ mol}^{-1}$	$\Delta_{\text{hyd}}H/\text{kJ mol}^{-1}$
Cl	75	347	367
SO <sub>4</sub> <sup>2-</sup>	200	1090	1035
K <sup>+</sup>	74	304	334
Li <sup>+</sup>	142	481	531
Ca <sup>2+</sup>	252	1515	1602
Al <sup>3+</sup>	538	4531	4715

<sup>a</sup> Ref. 59.

of the structure of amino acid–aluminum complexes cannot be found in literature, and the data obtained in this work does not also enable to properly infer the identity of those species, some insight into the molecular interactions behind the enhanced solubility effects of this cation can be provided by some reports. In fact, *ab initio* calculations of the aluminum and magnesium cations with amino acid residues have demonstrated that  $\text{Al}^{3+}$  binds much more tightly to the ligands than  $\text{Mg}^{2+}$ . Evidence for stronger Al–oxygen bonding has been reported and it has been shown that the addition of methyl groups stabilizes both metal complexes, being that effect significantly larger for the aluminum complex.<sup>26</sup> Moreover, potentiometric and NMR studies on the complexation of  $\text{Al}^{3+}$  with several amino acids have shown that, besides the negatively charged  $\text{COO}^-$  donors, the amino group can likewise participate in the binding of  $\text{Al}^{3+}$ .<sup>22</sup> These data suggest an enhanced stability of the aluminum ligands and partially explain the strong salting-in effects promoted by this cation. Further information on the speciation of this ion, and on the exact nature of the structures that result from the interactions established at the level of the carboxyl group is, however, absolutely required to find a definite molecular interpretation of these phenomena.

In sum, strongly hydrated polyvalent cations do not establish important (direct) interactions with the hydrophobic parts of the amino acids, but, due to their high charge density, are able to form charged complexes with the biomolecules, which are very soluble, promoting thus strong increases of their aqueous solubilities. The stronger the energy of hydration (the higher the charge), the more stable are these complexes and consequently the more pronounced are the effects. This behavior was observed for the magnesium ion<sup>14</sup> and is also experimentally found in this work for the  $\text{Ca}^{2+}$  and (more pronouncedly) for the  $\text{Al}^{3+}$  cations (Fig. 2, and Tables 2 and 3). These results are consistent with the molecular mechanism proposed before for the effect of salting-in inducing cations in aqueous solutions of amino acids.<sup>14</sup> On the other hand, weakly hydrated monovalent cations are not able to form those complexes, probably because their interaction with water is more favorable. They establish almost non significant interactions with the carboxyl group of the amino acids, and do not interact as well with their nonpolar moieties. Their solubility influence will be thus much less significant and will be ruled by the molecular mechanism by which salting-out anions operate.<sup>13</sup> This behavior was observed for  $\text{K}^+$  and  $\text{Na}^+$ ,<sup>14</sup> and comparatively, less pronounced solubility effects were observed in this work for the potassium and lithium salts (Fig. 2 and Tables 2 and 3). These interpretations are quantitatively supported by the interaction energies calculated in this work from the simulations, displayed in Table 5. As can be seen from the data, for the polyvalent cations the Coulomb terms of the energies corresponding to the (aa–cation) interactions are more favorable (less positive) than the (aa–water) values, while for the monovalent cations the opposite is observed. Further support can be obtained from density functional theory calculations for the relative stability of gas-phase complexes between metal ions and amino acids which have shown that the Gibbs energies of (ion–amino acid) systems are

Table 5 Values ( $\text{kJ mol}^{-1}$ ) of the Lennard-Jones (LJ) and Coulomb (Coul) terms of the energies calculated for the interactions (amino acid water), (amino acid anion) and (amino acid cation) for the different systems under study

Salt	Interaction	LJ	Coul
LiCl	aa water	45.4	2484.4
	aa anion	2.5	43.1
	aa cation	4.6	26.3
$\text{Li}_2\text{SO}_4$	aa water	22.6	2204.2
	aa anion	2.8	244.6
	aa cation	9.5	42.8
$\text{CaCl}_2$	aa water	48.9	1215.0
	aa anion	3.0	102.3
	aa cation	134.7	1733.1
$\text{K}_2\text{SO}_4$	aa water	16.8	2273.0
	aa anion	1.1	208.8
	aa cation	4.7	52.5
$\text{AlCl}_3$	aa water	26.6	336.9
	aa anion	18.4	92.4
	aa cation	358.4	5525.7
$\text{Al}_2(\text{SO}_4)_3$	aa water	109.5	1030.4
	aa anion	65.3	28.5
	aa cation	187.4	3549.5
Water	aa water	33.8	2560.6

much less positive in the case of divalent cations than of monovalent cations.<sup>66–68</sup>

**Cooperative/competitive effects.** The often neglected cation/anion, cooperativity/competition has proved to play an important role in the solubility effects promoted by inorganic salts in aqueous solutions of biomolecules, since the ions, depending on their properties, can have opposite or parallel effects.<sup>12,14</sup> For instance, while the (strong salting-in inducing) polyvalent cations will determine the direction of the solubility effect promoted by the salts, monovalent species will have a less significant influence. In both cases, however, the magnitude or the magnitude/direction (respectively) will be determined by the properties of their counterions. To elucidate the cooperative/competitive effects of the cation and anion on these systems, we compared the results obtained for some groups of systems.

First, comparing the experimental data for salts comprising strongly hydrated cations and weakly hydrated anions (Fig. 2, and Tables 2 and 3), it is observed that, in general, the magnitude of the salting-in decreases in the order  $\text{AlCl}_3 > \text{CaCl}_2$  (this work)  $\sim \text{MgCl}_2$ ,<sup>14</sup> consistently with the decrease observed in the RDF peaks referring to the ( $\text{O}_{\text{COO}^-}$ –cation) interactions (Fig. 5) and with previously reported data.<sup>14</sup> The intensity of these interactions is thus determined by the properties of the cation and dictates the magnitude of the solubility effect. On the other hand, when the salts combine a strongly hydrated cation and an also strongly hydrated anion, positioned in the extreme of the Hofmeister series, such as  $\text{SO}_4^{2-}$ , the presence of the latest leads to a decrease of the magnitude of the salting-in promoted by the cation, as experimentally observed for Ile (Fig. 2, and Tables 2 and 3). In agreement with the mechanism previously proposed,<sup>14</sup> there will be a competition between the interactions established by the cation and the anion, and its balance will determine the magnitude of the solubility effect. Finally,



analyzing the experimental results obtained for salts with weakly hydrated cations (Fig. 2, and Tables 2 and 3), a slight salting-out effect of Val and Ile is promoted by LiCl, while a stronger decrease in the aqueous solubility of both amino acids is observed in the presence of  $\text{Li}_2\text{SO}_4$ . As shown by the simulation data, the weakly hydrated  $\text{Li}^+$  and  $\text{Cl}^-$  ions do not significantly interact with the amino acids, justifying the small influence of the LiCl salt on the biomolecules aqueous solubilities. However, when the counterion is a strong salting-out agent such as sulfate, the anion dominates the mechanism and controls the solubility effect since almost no interactions are established by the cation.

**Interactions with water.** To further support the molecular interpretations proposed for the ion specific effects, one final note on the evidence obtained for the interaction pattern of the amino acids with water is worthy to point out. The RDFs calculated for water around the amino acid molecules depicted in Fig. 9 do not reveal significant differences in the water distribution around the terminal carbon atoms of Ile among the

different systems. Nevertheless, the nonpolar groups seem to be less hydrated in presence of  $\text{AlCl}_3$ , in agreement with the discussion above. As far as the  $\text{O}_{\text{COO}}-\text{H}_{\text{H}_2\text{O}}$  contact pairs are concerned, a decrease in the intensity of the RDF peaks in presence of the polyvalent cations is observed, while for the monovalent cations no significant difference is detected. This result is consistent with the inability of the latest to interact with the carboxyl group and with the strong affinity of the polyvalent cations with  $\text{COO}^-$ , demonstrated in this work. As proved before, the differences in the amino acid hydration are, at least partially, due to specific interactions between these molecules and the ions in solution.<sup>13,14</sup>

## 4. Conclusions

Novel experimental solubility measurements and MD simulations were performed to further elucidate the molecular phenomena underlying the cation specific effects in aqueous solutions of amino acids.

The results obtained enabled to clarify the influence of the charge of the cations and shows that the mechanisms by which monovalent cations operate in aqueous solutions of amino acids is different from that of polyvalent cations. Strongly hydrated polyvalent cations do not establish direct interactions with the nonpolar moieties of the amino acids, but are able to form charged complexes with the biomolecules, which are very soluble, promoting thus strong increase of their aqueous solubilities. The higher the charge, the more pronounced are the effects. The aluminum ion shows a particular behavior, which was thoroughly discussed. On the contrary, weakly hydrated singly charged cations are not able to form those complexes, and do not interact as well with their nonpolar moieties. Their solubility influence is thus much less significant and is ruled by the molecular mechanism by which salting-out anions operate.

The magnitude and direction of the solubility influence of the cations is determined by the properties of their counterions. Evidence for cooperative/competitive cation–anion interactions dependent on the nature of the ions was provided. However, to fully understand the mechanisms by which salt ions operate in biological media, further research is needed to disclose the exact nature of the structures that result from the interactions established between the ions and the biomolecules, particularly at the level of the carboxyl group.

Since the current studies have been performed in model amino acid natural media, the data here reported can be helpful to the understanding of other more complex biological environments, and thus be relevant to develop many areas of biochemistry and life sciences.

## Acknowledgements

This work was financed by national funding from FCT (Fundação para a Ciência e a Tecnologia) through the project PTDC/QUI-QUI/121520/2010, by FEDER funding through program COMPETE, and by national funding through FCT, in the ambit of project CICECO-FCOMP-01-0124-FEDER-037271 (Pest-C/CTM/LA0011/2013), LSRE/LCM (project PEST-C/EQB/

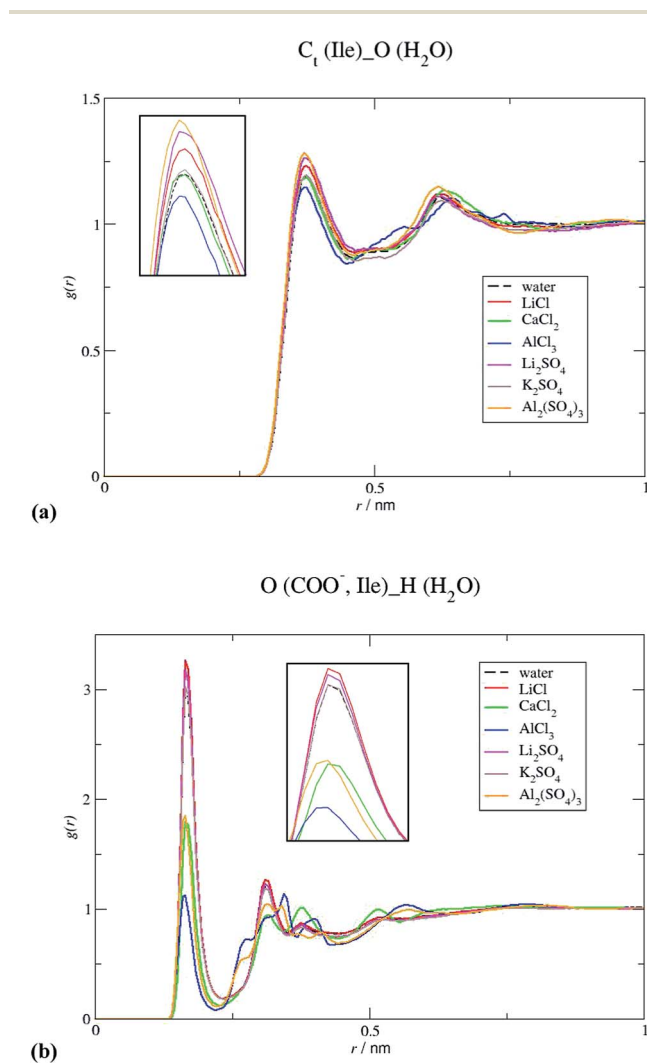


Fig. 9 Radial distribution functions of the oxygen and hydrogen atoms of water around selected groups of Ile: (a) terminal carbon and (b) carboxylate.

LA0020/2013) and project NORTE-07-0162-FEDER-000050. We also acknowledge FCT for the postdoctoral grant SFRH/BPD/44926/2008 to LINT. JRBG acknowledges FCT for the 2012 FCT Investigator Program position.

## References

- 1 P. Jungwirth and B. Winter, *Annu. Rev. Phys. Chem.*, 2008, **59**, 343.
- 2 S. Mader, *Biology*, McGraw Hill, New York, 9th edn, 2007.
- 3 F. Chiti and C. M. Dobson, *Annu. Rev. Biochem.*, 2006, **75**, 333.
- 4 J. S. Dennis, *Nature*, 2003, **426**, 900.
- 5 Y. J. Zhang, S. Furyk, D. E. Bergbreiter and P. S. Cremer, *J. Am. Chem. Soc.*, 2005, **127**, 14505.
- 6 W. Kunz, J. Henle and B. W. Ninham, *Curr. Opin. Colloid Interface Sci.*, 2004, **9**, 19.
- 7 M. W. Q. Washabaugh and K. D. Collins, *J. Biol. Chem.*, 1986, **261**, 2477.
- 8 M. Bostrom, D. R. M. Williams and B. W. Ninham, *Biophys. J.*, 2003, **85**, 686.
- 9 J. D. Batchelor, A. Olteanu, A. Tripathy and G. J. Pielak, *J. Am. Chem. Soc.*, 2004, **126**, 1958.
- 10 Y. J. Zhang, S. Furyk, L. B. Sagle, Y. Cho, D. E. Bergbreiter and P. S. Cremer, *J. Phys. Chem. C*, 2007, **111**, 8916.
- 11 Y. J. Zhang and P. S. Cremer, *Curr. Opin. Colloid Interface Sci.*, 2006, **10**, 658.
- 12 W. J. Xie and Y. Q. Gao, *J. Phys. Chem. Lett.*, 2013, **4**, 4247.
- 13 L. I. N. Tomé, M. Jorge, J. R. B. Gomes and J. A. P. Coutinho, *J. Phys. Chem. B*, 2010, **114**, 16450.
- 14 L. I. N. Tomé, S. P. Pinho, M. Jorge, J. R. B. Gomes and J. A. P. Coutinho, *J. Phys. Chem. B*, 2013, **117**, 6116.
- 15 F. Hofmeister, *Arch. Exp. Pathol. Pharmacol.*, 1888, **XXIV**, 247.
- 16 E. Rezabal, J. M. Mercero, X. Lopez and J. M. Ugalde, *J. Inorg. Biochem.*, 2006, **100**, 374.
- 17 L. Ronconi and P. J. Sadler, *Coord. Chem. Rev.*, 2008, **252**, 2239.
- 18 T. Dudev and C. Lim, *Acc. Chem. Res.*, 2007, **40**, 85.
- 19 J. P. André and H. R. Macke, *J. Inorg. Biochem.*, 2003, **97**, 315.
- 20 P. Djurdjevic, R. Jelic, L. Kjkovic and M. Cvijovic, *Monatsh. Chem.*, 2006, **137**, 717.
- 21 S. J. Karlik, E. Tarien, G. A. Elgavish and G. L. Eichhorn, *Inorg. Chem.*, 1983, **22**, 525.
- 22 T. Kiss, I. Sóvágó, I. Tóth, A. Lakatos, R. Bertani, A. Tapparo, G. Bombi and R. B. Martin, *J. Chem. Soc., Dalton Trans.*, 1997, 1967.
- 23 P. Djurdjevic, M. Cvijovic, V. Pavelkic and J. Zakrzewska, *Spectrosc. Lett.*, 2005, **38**, 617.
- 24 C. A. Alfrey, *Toxicity of Detrimental Metal Ions. Aluminium*, M. Dekker, New York, 1995.
- 25 G. Berthon, *Coord. Chem. Rev.*, 2002, **228**, 319.
- 26 J. M. Mercero, J. E. Fowler and J. M. Ugalde, *J. Phys. Chem. A*, 1998, **102**, 7006.
- 27 W. R. Harris, G. Berthon, J. P. Day, C. Exley, T. P. Flaten, W. F. Forbes, T. Kiss, C. Orvig and P. F. Zatta, *J. Toxicol. Environ. Health*, 1996, **48**, 543.
- 28 M. Hollósi, Z. M. Shen, A. Perczel and G. D. Fasman, *Proc. Natl. Acad. Sci. U. S. A.*, 1994, **91**, 4902.
- 29 T. Kiss, *Arch. Gerontol. Geriatr.*, 1995, **21**, 99.
- 30 D. F. Parsons, M. Bostrom, P. Lo Nostro and B. W. Ninham, *Phys. Chem. Chem. Phys.*, 2011, **13**, 12352.
- 31 R. Carta and G. Tola, *J. Chem. Eng. Data*, 1996, **41**, 414.
- 32 M. K. Khoshkbarchi and J. H. Vera, *Ind. Eng. Chem. Res.*, 1997, **36**, 2445.
- 33 R. Carta, *J. Chem. Thermodyn.*, 1998, **30**, 379.
- 34 A. A. Pradhan and J. H. Vera, *J. Chem. Eng. Data*, 2000, **45**, 140.
- 35 P. Ramasami, *J. Chem. Eng. Data*, 2002, **47**, 1164.
- 36 L. A. Ferreira, E. A. Macedo and S. P. Pinho, *Ind. Eng. Chem. Res.*, 2005, **44**, 8892.
- 37 L. A. Ferreira, E. A. Macedo and S. P. Pinho, *Fluid Phase Equilib.*, 2007, **255**, 131.
- 38 L. A. Ferreira, E. A. Macedo and S. P. Pinho, *J. Chem. Thermodyn.*, 2009, **41**, 193.
- 39 F. I. El-Dossoki, *J. Solution Chem.*, 2010, **39**, 1311.
- 40 T. Arakawa and S. N. Timasheff, *Biochemistry*, 1984, **23**, 5912.
- 41 M. Lund, L. Vrbka and P. Jungwirth, *J. Am. Chem. Soc.*, 2008, **130**, 11582.
- 42 B. Basak, U. K. Bhattacharyya, A. Sinhababu and S. Laskar, *Appl. Biochem. Biotechnol.*, 1994, **49**, 281.
- 43 M. P. Breil, J. M. Mollerup, E. S. J. Rudolph, M. Ottens and L. A. M. van der Wielen, *Fluid Phase Equilib.*, 2004, **215**, 221.
- 44 P. Venkatesu, M.-J. Lee and H.-M. Lin, *Biochem. Eng. J.*, 2006, **32**, 157.
- 45 B. Hess, C. Kutzner, D. van der Spoel and E. Lindahl, *J. Chem. Theory Comput.*, 2008, **4**, 435.
- 46 R. W. Hockney and S. P. J. Goel, *Comput. Phys.*, 1974, **14**, 148.
- 47 S. Nosé, *Mol. Phys.*, 1984, **52**, 255.
- 48 W. G. Hoover, *Phys. Rev. A*, 1985, **31**, 1695.
- 49 M. Parrinello and A. Rahman, *J. Appl. Phys.*, 1981, **52**, 7182.
- 50 U. Essman, L. Perela, M. L. Berkowitz, T. Darden, H. Lee and L. G. Pederson, *J. Chem. Phys.*, 1995, **103**, 8577.
- 51 B. Hess, H. Bekker, H. J. C. Berendsen and J. G. E. M. Fraaije, *J. Comput. Chem.*, 1997, **18**, 1463.
- 52 H. J. C. Berendsen, J. R. Grigera and T. P. Straatsma, *J. Phys. Chem.*, 1997, **91**, 6269.
- 53 J. Aqvist, *J. Phys. Chem.*, 1990, **94**, 8021.
- 54 J. Chandrasekhar, D. C. Spellmeyer and W. L. Jorgensen, *J. Am. Chem. Soc.*, 1984, **106**, 903.
- 55 W. R. Cannon, B. M. Pettitt and J. A. McCammon, *J. Phys. Chem.*, 1994, **98**, 6225.
- 56 T. M. C. Faro, G. P. Thim and M. S. Skaf, *J. Chem. Phys.*, 2010, **132**, 114509.
- 57 J. Heyda, T. Hrobárik and P. Jungwirth, *J. Phys. Chem. A*, 2009, **113**, 1969.
- 58 D. L. Nelson and M. M. Cox, *Lehninger Principles of Biochemistry*, Worth Publishers, New York, 2008.
- 59 Y. Marcus, *Ion Properties*; Marcus Dekker, New York, 1997.
- 60 S. Shahriari, C. M. S. S. Neves, M. G. Freire and J. A. P. Coutinho, *J. Phys. Chem. B*, 2012, **116**, 7252.
- 61 G. Fuser and A. Steinbuchel, *Biomacromolecules*, 2005, **6**, 1367.
- 62 J. Kherb, S. C. Flores and P. S. Cremer, *J. Phys. Chem. B*, 2012, **116**, 7389.

- 63 J. Tian, Y. Yin, H. Sun and X. Luo, *J. Magn. Reson.*, 2002, **159**, 137.
- 64 T. Dudev and C. Lim, *Chem. Rev.*, 2003, **103**, 773.
- 65 J. P. Greenstein and M. Wintz, *Chemistry of the amino acids*, John Wiley & Sons, New York, 1961, vol. 1.
- 66 M. Remko, D. Fitz and B. M. Rode, *J. Phys. Chem. A*, 2008, **112**, 7652.
- 67 M. Remko, D. Fitz and B. M. Rode, *Amino Acids*, 2010, **39**, 1309.
- 68 M. Remko and B. M. Rode, *J. Phys. Chem. A*, 2006, **110**, 1960.